



Published in final edited form as:

*Cell*. 2009 January 23; 136(2): 337–351. doi:10.1016/j.cell.2008.11.051.

## Digital signaling and hysteresis characterize Ras activation in lymphoid cells

Jayajit Das<sup>1</sup>, Mary Ho<sup>4</sup>, Julie Zikherman<sup>5</sup>, Christopher Govern<sup>1</sup>, Ming Yang<sup>1</sup>, Arthur Weiss<sup>5,6,\*</sup>, Arup K. Chakraborty<sup>1,2,3,\*</sup>, and Jeroen P. Roose<sup>4,\*</sup>

<sup>1</sup> Department of Chemical Engineering, Massachusetts Institute of Technology, 77 Massachusetts Avenue, Cambridge, MA 02139

<sup>2</sup> Department of Chemistry, Massachusetts Institute of Technology, 77 Massachusetts Avenue, Cambridge, MA 02139

<sup>3</sup> Department of Biological Engineering, Massachusetts Institute of Technology, 77 Massachusetts Avenue, Cambridge, MA 02139

<sup>4</sup> Department of Anatomy, University of California, 513 Parnassus, San Francisco, CA 94143

<sup>5</sup> Department of Medicine, Division of Rheumatology, University of California, 513 Parnassus, San Francisco, CA 94143

<sup>6</sup> Howard Hughes Medical Institute, University of California, 513 Parnassus, San Francisco, CA 94143

### Abstract

Activation of Ras proteins underlies functional decisions in diverse cell types. Two molecules, RasGRP and SOS, catalyze Ras activation in lymphocytes. Binding of active Ras to SOS' allosteric pocket markedly increases SOS' activity establishing a positive feedback loop for SOS-mediated Ras activation. Integrating *in silico* and *in vitro* studies, we demonstrate that digital signaling in lymphocytes (cells are “on” or “off”) is predicated upon feedback regulation of SOS. SOS' feedback loop leads to hysteresis in the dose-response curve, which can enable a capacity to sustain Ras activation as stimuli are withdrawn and exhibit “memory” of past encounters with antigen. Ras activation via RasGRP alone is analog (graded increase in amplitude with stimulus). We describe how complementary analog (RasGRP) and digital (SOS) pathways act on Ras to efficiently convert analog input to digital output. Numerous predictions regarding the impact of our findings on lymphocyte function and development are noted.

### INTRODUCTION

Activated Ras proteins regulate several cellular processes by acting on many substrates to affect signaling through diverse pathways (e.g., the MAPK pathway) (Campbell et al., 1998; Mor and Philips, 2006). Membrane-bound Ras proteins shuttle between inactive (GDP-bound) and active (GTP-bound) states. RasGDP binding to guanine nucleotide exchange factors (GEFs) results in nucleotide release, enabling nucleotide-free Ras to bind more abundant cellular GTP

\*corresponding authors: AW: aweiss@medicine.ucsf.edu; AC: arupc@mit.edu; JR: jeroen.roose@ucsf.edu.

**Publisher's Disclaimer:** This is a PDF file of an unedited manuscript that has been accepted for publication. As a service to our customers we are providing this early version of the manuscript. The manuscript will undergo copyediting, typesetting, and review of the resulting proof before it is published in its final citable form. Please note that during the production process errors may be discovered which could affect the content, and all legal disclaimers that apply to the journal pertain.

(Campbell et al., 1998). The intrinsic GTPase activity of Ras is enhanced by Ras GTPase activating proteins (RasGAPs) that promote Ras deactivation (Campbell et al., 1998).

Ras activation is important for the development of T and B lymphocytes and for their effector functions directed against invading pathogens (Genot and Cantrell, 2000). Antigen receptor stimulation of lymphocytes triggers uniquely high levels of Ras activation (Genot and Cantrell, 2000). Two families of RasGEFs are well-studied in lymphocytes: RasGRP1 and RasGRP3 (Ras guanyl nucleotide release protein) and SOS1 and SOS2 (Son of Sevenless) (Ebinu et al., 2000; Roose et al., 2005; Roose et al., 2007). RasGRP proteins, mainly restricted to the nervous and hematopoietic systems, are activated by binding to membrane localized diacylglycerol and by phosphorylation by protein kinase C (see Figures 2A and 4A). SOS proteins are ubiquitous and are recruited to sites of receptor or adaptor tyrosine phosphorylation. SOS' activity is regulated by membrane localization and is greatly accelerated upon binding of active RasGTP to a non-catalytic (allosteric) site. The functional consequences of such feedback regulation of SOS' activity, and its interplay with the other GEF, RasGRP, were unknown.

An important issue in cell biology is to understand how cells respond in a decisive manner (digital) to the graded (analog) input of increasing amounts of receptor stimulation. Employing synergistic *in silico* and *in vitro* methods, we find that signaling in a population of lymphocytes is digital in character; i.e., a bimodal response emerges as stimulus is increased past a threshold. Digital signaling in individual cells requires SOS-mediated Ras activation. A further unanticipated characteristic of Ras activation via SOS is hysteresis in the dose-response curve; i.e., the response to the same stimulus dose depends upon whether the prevailing level of stimulus is achieved by increasing or decreasing the stimulus from its previous value. Our results suggest that bimodal responses and hysteresis also provide a mechanism for short-term molecular "memory", making it easier to activate membrane-proximal signaling in previously stimulated cells. This may enable T lymphocytes to integrate signals from serial encounters with rare antigen-bearing cells.

We find that Ras activation via RasGRP alone increases in a graded fashion with stimulus (analog), and does not exhibit hysteresis. This is because, unlike SOS, RasGRP's activity is not regulated by a positive feedback loop. Our results show how tuning the interplay between two complementary digital and analog signaling modules that activate the same substrate (Ras) leads to more efficient digital responses than if the digital pathway alone was employed. This may be a principle used broadly in biology.

Positive feedback regulation is one of many non-linear mechanisms that can result in "digital" responses of gene regulation programs and signaling networks (Barkai and Leibler, 2000; Bhalla and Iyengar, 1999; Elf and Ehrenberg, 2004; Ferrell, 2002; Kholodenko et al., 2002; McAdams and Arkin, 1997). We describe an example of how positive feedback regulation of a signaling module embedded in a complex signaling network leads to functionally important consequences in cells that orchestrate adaptive immunity. The concepts revealed by our study lead to a number of testable predictions pertinent to lymphocyte development and their ability to be activated *in vivo* by small doses of stimulatory ligands.

## RESULTS

### A positive feedback loop that regulates SOS activity results in digital signaling

Stimulated tyrosine kinase receptors (e.g., growth factor receptors, T cell receptors), recruit SOS to the plasma membrane by the adapter molecule, Grb2 (Genot and Cantrell, 2000). The Rem and Cdc25 domains in SOS are required for its GEF catalytic activity (Figure 1A), and we refer to them together as  $SOS_{cat}$  (SOS catalytic domain). SOS itself has very low GEF activity. Crystallographic and biochemical studies as well as experiments with cell lines show

that the activity of  $SOS_{cat}$  is strongly influenced by a second Ras binding site which is distal to the GEF catalytic site (Margarit et al., 2003). Binding of RasGDP to this allosteric pocket results in a 5-fold increase in GEF activity, whereas binding of RasGTP effects a much larger (~ 75-fold) increase (Freedman et al., 2006; Sondermann et al., 2004). Thus, SOS-mediated Ras activation involves positive feedback regulation by its own catalytic product, RasGTP (Figure 1A).

The activity of full-length SOS is inhibited by both N-terminal and C-terminal regions that flank  $SOS_{cat}$  (Figure S21A). Recruitment of SOS to the plasma membrane results in conformational changes that relieve this inhibition and allow RasGDP to bind to SOS' catalytic site (Corbalan-Garcia et al., 1998). In agreement, expression of  $SOS1_{cat}$  without these flanking sequences results in Ras signaling without the need for membrane targeting or external stimulus (Roose et al., 2007). We explored the consequences of positive feedback regulation of SOS by developing a mathematical model for the signaling module in Figure 1B wherein  $SOS_{cat}$  is uninhibited.

We first ignored stochastic fluctuations (Kampen, 1992) in the number of molecules participating in signaling, and developed a deterministic model describing the temporal evolution of the most probable number (or concentration) of the proteins involved in Ras activation via  $SOS_{cat}$  (Figure 1B). Table 1 summarizes the values of rate parameters that appear in the equations (Procedures). Only the ratios of certain parameters had been measured. Varying the individual parameters by factors of at least ten while keeping the ratio fixed did not affect the qualitative results (Figures S2–S4).

Figure 1C shows the theoretical steady-state dose-response curve for Ras activity as the amount of  $SOS_{cat}$  ( $\alpha$ ) is varied. For low or high levels of  $SOS_{cat}$ , there is one possible state characterized by low or high levels of active Ras, respectively. However, for intermediate levels of  $SOS_{cat}$ , three states of Ras activity are possible. The states shown in blue are unstable to small perturbations, and these states could exist only fleetingly. Therefore, for intermediate levels of  $SOS_{cat}$ , two possible dominant states of Ras activity could be simultaneously observed; i.e., a bistability is predicted. As the amount of  $SOS_{cat}$  is increased, the system could follow the lower stable branch until this was no longer possible, and then there would be a large jump in Ras activity (at point A). Thus, the dose-response curve could be very sharp. Importantly, bistability and the concomitant sharp threshold are abrogated if the positive feedback loop regulating SOS' GEF activity is removed from the model (green line in Figure 1D and S2E).

Formulas obtained from a detailed analytical study (Supplement, Section VI) suggest that, in addition to feedback regulation of SOS, the minimal requirements for bistable Ras activity are: 1] catalytic Ras activation by SOS, with RasGTP bound to the allosteric site and 2] catalytic deactivation of RasGTP by RasGAPs. These features are true. The analytical treatment of simplified models also supports our numerical parameter sensitivity studies which show that our qualitative results are robust to wide variations in parameters as long as the basic ingredients described above are present.

We then investigated the potential effect of Ras activation via RasGRP1 on the bistable Ras activity driven by  $SOS_{cat}$ . A GEF, RasGRF, which is structurally related to RasGRP, is not dependent on feedback regulation by Ras (Freedman et al., 2006). So, we assumed that Ras is activated by RasGRP without feedback, and used the measured rate parameters for RasGRF since those for RasGRP are unknown. As shown in Figure 1E, bistability and sharp responses are predicted to disappear if RasGRP levels (or activity) are very high. This is because RasGRP activity, which is not subject to feedback regulation can convert most Ras molecules to its active form before the SOS feedback loop is engaged. Figure 1E also shows that low levels of RasGRP activity reduce the threshold for  $SOS_{cat}$  ( $\alpha$ ) to induce a sharp response. We show later

that this is because absence of RasGRP makes it difficult to ignite the positive feedback loop regulating SOS' GEF activity. These results suggest that an optimal level of expression or activity of RasGRP, the analog route to Ras activation, enables efficient deployment of feedback regulation of SOS which leads to bistability.

To explore the manifestations of these characteristics of Ras activation in lymphocytes (where stochastic variations between stimulated cells can be important), we carried out stochastic computer simulations of signaling events that might occur in lymphocytes (Figure 2A). The simulations were carried out using the Gillespie algorithm (Gillespie, 1977), which has been used profitably to study biological systems that exhibit multi-stability (Elf and Ehrenberg, 2004; McAdams and Arkin, 1997). Parameters not listed in Table 1 needed to carry out the simulations are provided in the supplement. The qualitative features of the results are robust to variations in unknown parameters over wide ranges (Tables S6–S8, Figures S5–S12). The purpose of our *in silico* studies was not quantitative recapitulation of known data, but to provide qualitative mechanistic insights that can be tested experimentally.

We carried out stochastic calculations using the amount of  $SOS_{cat}$  as a surrogate for the level of receptor stimulation. Many replicate dynamic simulations were carried out and levels of RasGTP at various time points were recorded (see Figure S30 for examples). Each simulation corresponds to assaying an individual lymphocyte. The combined results for all such *in silico* “cells” at a particular time point are displayed (Figure 2B). For low levels of  $SOS_{cat}$ , all simulations result in low levels of RasGTP, resulting in a single corresponding peak in the histogram. As  $SOS_{cat}$  is increased, this peak does not gradually move to higher values of RasGTP. Rather, beyond a threshold value of  $SOS_{cat}$ , a second peak corresponding to a much higher level of RasGTP emerges; the histogram is bimodal (Figure 2B). Thus, the sharp threshold and bistability shown in Figure 1C are manifested as digital signaling. The prediction is that lymphocytes are either “on” or “off” with regard to Ras activation.

To test these predictions, we used a Jurkat T cell line into which different amounts of  $SOS1_{cat}$  and GFP were transfected together (Roose et al., 2007). Individual cell assays are required to compare experimental results with the histograms shown in Figure 2B. Analysis of active Ras for individual cells in a population is not possible in this transfection experiment, and so we examined upregulation of a cell surface activation marker CD69 by individual cells using flow cytometry. CD69 levels correlate with the strength of Ras-ERK signaling (Roose et al., 2007), but activation of signaling molecules downstream of Ras could be influenced by feedback regulation of modules such as the MAPK pathway (Ferrell, 2002; Kholodenko et al., 2002). We will address this issue directly below.

Low or high levels of  $SOS1_{cat}$  expression led to unimodal cell populations with low or high levels of CD69 induction (Figure 2C and S21B). Intermediate levels of  $SOS1_{cat}$  (red) induced a bimodal CD69 expression pattern in wild-type Jurkat T cells (Figure 2C).  $SOS1_{cat}$ -induced bimodality was not observed for a control marker that is Ras-unresponsive (Figure S21C). These results in cells mirror the predictions of the computer simulations in that signaling is digital. We next tested the hypothesis emerging from our calculations (Figure 1C and Figure S2E) that the origin of digital signaling is feedback regulation of SOS-mediated Ras activation.

Experiments carried out with RasGRP1-deficient JPRM441 cells indicate the importance of this feedback loop. In contrast to wildtype cells (Figure 2C), intermediate levels of  $SOS1_{cat}$  induced high CD69 expression levels in very few JPRM441 cells (13% in Figure 3A, top row). Similarly, intermediate levels of  $SOS_{cat}$  did not generate a bimodal response in computer simulations of the RasGRP deficient state (Figure 3B). Basal RasGRP1-mediated activation of Ras is not subject to feedback regulation, but can “ignite” the SOS feedback loop (Roose et al., 2007) by providing RasGTP which can bind SOS' allosteric pocket and increase its activity

75-fold. Consistent with our computational results (Figure 1E), in RasGRP-deficient JPRM441 cells, lower basal levels of RasGTP make it more difficult to ignite the SOS feedback loop. Sufficiently high levels of  $SOS_{cat}$  can induce bimodal responses without RasGRP1 (Figures 3A, 3B, 1E and S22) because RasGTP produced by the GEF activity of  $SOS_{cat}$  with RasGDP bound to the allosteric pocket can ultimately prime SOS' feedback loop.

The computer simulation results suggested that a bimodal response would re-emerge in RasGRP-deficient cells for intermediate levels of  $SOS1_{cat}$  if exogenous RasGTP molecules that bind to SOS' allosteric pocket were added. To test this, we introduced Ras molecules like H-RasV12C40 (Roose et al., 2007) or H-RasG59E38 (Boykevisch et al., 2006) that are predominantly GTP loaded (because of the V12 or G59 mutation) and thus bind SOS' allosteric pocket to increase GEF activity. These molecules also contain a second mutation (C40 or E38) that impairs binding to RAF and so do not directly activate the RAF-MEK-ERK-CD69 pathway; i.e., downstream pathways must be activated by endogenous Ras molecules.

In this type of assay, not all transfected cells start to express  $SOS1_{cat}$  synchronously and  $SOS1_{cat}$  expressing cells transit from low CD69 to high CD69 expression. It is therefore difficult to ascertain whether the response is bimodal or not by visual inspection. We adapted Hartigan's test (Hartigan, 1985), which allows for a qualitative determination of whether a response in a population of cells is bimodal or unimodal. The generated histograms were divided into 120 equal portions and the mean fluorescence of CD69 and the number of cells in each portion were determined. Hartigan's test confirmed that intermediate levels of  $SOS1_{cat}$  when combined with H-RasG59E38 but not wt H-Ras restored bimodal signaling in RasGRP-deficient cells (Figure 3C, bottom row: B with  $p < 0.01$ ). The same level of  $SOS1_{cat}$  or H-RasG59E38 alone also did not result in high CD69 expression (Figure 3C, top row, unimodal; U:  $p < 0.01$ ). Importantly, when the allosteric pocket in  $SOS_{cat}$  is mutated ( $SOS1_{cat}$ -W729E), so that it can no longer interact with nucleotide-associated Ras proteins, adding H-RasG59E38 does not result in a bimodal pattern of signaling (Figure 3C, bottom row). Similar results were obtained with H-RasV12C40 (data not shown). Modeling this cell biological experiment is in concurrence with these results (Figure 3D). Therefore, the digital signaling we observe for ERK-CD69 signaling requires feedback regulation of SOS-mediated Ras activation.

There are two possible reasons for why digital signaling in lymphocytes originates in SOS-mediated Ras activation: (i) Ignition of the SOS feedback loop is necessary for generating sufficiently high levels of RasGTP required to prime downstream feedback loops that cause digital signaling (e.g., those associated with the MAPK pathway (Bhalla and Iyengar, 1999; Ferrell, 2002; Kholodenko et al., 2002)). (ii) Digital signaling is controlled by feedback regulation of Ras activation by SOS. Whereas signaling is undoubtedly influenced by feedback regulation of downstream signaling modules, results described below suggest that, in lymphocytes, the latter scenario is true.

### Receptor stimulation results in digital signaling with SOS and analog responses with RasGRP alone

The strength of lymphocyte receptor stimulation impacts outcomes (e.g., T cell activation, thymocyte development (Starr et al., 2003)). Therefore, we studied how SOS and RasGRP influence cellular responses as the amount of stimulatory ligands is varied.

We studied a simplified computational model for processes upstream of Ras activation (See section III, supplement). In short (see Figure 4A), receptor stimulation and phosphorylation generates activated ZAP-70 molecules. Activated-ZAP-70 phosphorylates the adaptor molecule LAT, which recruits both PLC $\gamma$  and Grb2/SOS. PLC $\gamma$  is then phosphorylated, and this generates IP3 and DAG. Induced DAG enhances RasGRP recruitment and activation. We

do not incorporate cooperative effects associated with Grb2/SOS recruitment to LAT (Houtman et al., 2006). Including this feature would lead to sharper cellular responses (Prasad).

For weak receptor stimulation, as might occur under physiologic antigen receptor stimulation (Figure 4B), wildtype systems that have low initial levels of active Ras exhibit a bimodal pattern of signaling after a short time which ultimately becomes a unimodal distribution with high RasGTP (Figure 4B, left column). For very strong stimulation, a unimodal state of high RasGTP is rapidly reached (Figure 4C, left column). Without RasGRP, signaling is inhibited. Importantly, without SOS such systems demonstrate a graded response, indicating the analog character of RasGRP-mediated Ras activation (Figure 4C, middle column). Changing the values of the parameters (e.g., the numbers of RasGRP and SOS molecules) used to obtain the results shown in Figure 4 does not lead to qualitative changes (Tables S12–S13, Figures S13–S20).

To test these predictions, we determined the pattern of ERK phosphorylation in individual cells. First, 20,000 Jurkat T cells were either stimulated via the TCR or by PMA. The latter mimics a DAG-PKC-RasGRP pathway, but does not target SOS. Engagement of the TCR generated a unimodal P-ERK response at early timepoints that transitioned to a bimodal response at three minutes after stimulation (Figure 5A). In contrast, even strong stimulation via PMA never induced a bimodal ERK phosphorylation pattern and, instead, exhibited an analog response (Figure 5B).

Experiments with cells wherein genes of interest were deleted further support these results. Peripheral T cells do not develop in RasGRP1 deficient mice (Dower et al., 2000) and a selective  $SOS1^{-/-}SOS2^{-/-}$  peripheral T cell model to circumvent lethality due to  $SOS1$  deficiency has not been generated (Wang et al., 1997). Therefore, we used a chicken DT40 B cell line in which pertinent genes have been genetically inactivated (Roose et al., 2007). We analyzed the ERK phosphorylation pattern of 20,000 cells (wildtype,  $SOS1^{-/-}SOS2^{-/-}$ , and  $RasGRP1^{-/-}RasGRP3^{-/-}$ ) that were stimulated with increasing levels of B cell receptor (BCR) crosslinking-M4 monoclonal antibody.

Wildtype cells stimulated by low levels of M4, mimicking physiological lymphocyte stimulation by antigen, exhibited a bimodal pattern of ERK activation at the 3 and 10 minutes time points (Figure 5C “WEAK” and S24). Hartigan’s tests (Hartigan, 1985) confirmed that the response is bimodal. In contrast,  $SOS1^{-/-}SOS2^{-/-}$  DT40 B cells do not exhibit bimodal distributions at any time point regardless of stimulus level (Figure 5C, middle column). Thus, without SOS, signaling is analog in character regardless of strength of stimulus. Furthermore, while PMA-induced responses were severely impaired in  $RasGRP1^{-/-}RasGRP3^{-/-}$  cells (Figure 5D, right column), PMA induced very similar analog patterns of ERK phosphorylation in wildtype and  $SOS1^{-/-}SOS2^{-/-}$  DT40 B cells (Figure 5D, left and middle columns). These results reveal analog ERK responses from RasGRP-induced Ras activation, and that there is no intrinsic defect preventing  $SOS1^{-/-}SOS2^{-/-}$  DT40 B cells from turning on the Ras-ERK pathway.

This behavior in cell lines was mirrored in primary CD4 positive peripheral T cells. *Ex vivo* TCR stimulation of primary cells results in a digital pattern of ERK phosphorylation (Figure 5E), but PMA stimulation results in analog signaling (Figure 5F).

Thus, in Jurkat T cells, DT40 B cells, and primary lymph node T cells digital signaling requires engagement of the SOS pathway for Ras activation (Figs. 2–5). Notably, for all systems, the ERK response to PMA stimulation was analog at all doses tested, including those that generate high levels of RasGTP. This implies that the predicted analog Ras response in the absence of SOS (Fig. 4C, middle column) is not translated to digital responses by downstream signaling modules. If ignition of the positive feedback loop associated with SOS-mediated Ras activation

only served to generate high levels of RasGTP that can stimulate digital signaling in a downstream module such as the MAPK pathway, a bimodal pattern of ERK activation should have been observed upon strong PMA stimulation. Since this is not so (Figure 5B and D), our results suggest that the digital signaling we observe for ERK and CD69 is not only predicated on positive feedback regulation of SOS-mediated Ras activation (Figure 3 and 4C), but is controlled by it.

### Prediction of hysteresis in Ras activation

Due to technical limitations, we are not able to carry out single cell assays of Ras activity. However, another related, but unanticipated characteristic that derives from our model, hysteresis, can be assessed by measuring Ras activation at the population level. Hysteresis is a direct consequence of bistability due to positive feedback regulation of SOS-mediated Ras activation (Figure 1), and the phenomenon and its biochemical origin is shown in Figure 6.

When previously unactivated cells are stimulated, RasGTP levels are low. Hence, the allosteric site of most SOS molecules is occupied by RasGDP and SOS' GEF activity is low. Increasing stimulus results in more RasGTP production, and an increase in the number of SOS molecules with RasGTP bound to the allosteric pocket, resulting in ignition of the positive feedback loop and a sharp increase in active Ras levels. These processes result in the black dose-response curve in Figure 6A, which is obtained from computer simulations where the initial RasGTP levels were set to zero.

A very different dose-response curve (red curve in Figure 6A) is predicted by computer simulations where the initial RasGTP level was set to a large value, and then the response to smaller stimulus levels were calculated. This is the predicted dose-response for cells that are first robustly stimulated such that a high RasGTP level is realized, then the stimulus is quickly reduced (as in removal of antigen), and the response assessed after a time period that is sufficient for a new active Ras level to be established. When cells that have been previously robustly activated are exposed to lower stimulus levels, most SOS molecules have RasGTP bound to the allosteric site and are characterized by high GEF activity. So, for the same stimulus level (or SOS targeted to the membrane), previously stimulated cells will exhibit a higher level of active Ras than previously unstimulated cells because in the former situation SOS is a more active enzyme. Concomitantly, the threshold stimulus required for robust Ras activation shifts to lower values (Figure 6A and B) for previously stimulated cells. However, this hysteretic effect will only be manifested for a finite period of time. Ultimately, RasGTP molecules bound to the allosteric site of SOS in previously stimulated cells will be displaced by RasGDP molecules as the amount of RasGTP in the cell declines because of lower stimulus levels. If the second stimulus level falls below a threshold, this process occurs very rapidly, and this is why hysteresis is not predicted for weak receptor stimulation.

### SOS-dependent hysteresis in Ras activation

Experimental results for Jurkat T cells and DT40 B cells (Figures 6C–L) demonstrate the predicted hysteresis in Ras activation, and that it is due to the feedback loop associated with SOS and not due to feedback from downstream signaling modules.

Stimulation of Jurkat T cells using a maximal dose of TCR crosslinking antibody results in near maximal Ras activation after 3 minutes of stimulation (Figure S27A). Cells were also exposed to increasing concentrations of Src kinase inhibitor (PP2) to inhibit Lck (see Figure 4A) and interrupt signaling events upstream of Ras activation in a dose-dependent manner. PP2 was introduced simultaneously with the stimulus ( $t=0$  min) or after cells reached maximal levels of RasGTP ( $t=3$  min). RasGTP was analyzed at three minutes for PP2 added at  $t=0$  min. If PP2 was added at  $t=3$  min, RasGTP was assayed at seven minutes, thereby allowing a new

balance with the reduced stimulus to be established. Computer simulations (Figure S27D) show that this protocol should allow us to test whether hysteresis occurs at the level of Ras as predicted in Figure 6A.

Figure 6C shows that TCR-induced RasGTP levels in wildtype Jurkat cells decrease when PP2 is added simultaneously with the stimulus, demonstrating a dependence on Src kinases (or stimulus level) for RasGTP generation that is akin to the black curve in Figure 6A for previously unstimulated cells. However, when PP2 is added at three minutes (stimulus lowered after stimulation), RasGTP levels are high at seven minutes even at high doses of PP2. This is akin to the red curve in Figure 6A, and demonstrates hysteresis because, in previously stimulated cells, RasGTP levels are relatively high between three and seven minutes in spite of a lower stimulus. After a sufficiently long time, as predicted, hysteresis is not observed (data not shown).

Importantly, these effects were not determined by feedback loops originating downstream of Ras. Preloading of cells with MEK1/2 inhibitor, U0126, efficiently blocks MEK and ERK phosphorylation but allows for RasGTP generation, albeit with slightly delayed kinetics (Figure S27A), but hysteresis was still observed (Figure 6D).

We also tested the prediction that SOS-mediated Ras activation underlies hysteresis by using the doubly SOS deficient DT40 cells. Maximal BCR crosslinking leads to similarly high-levels of RasGTP at three minutes in wildtype and  $SOS1^{-/-}SOS2^{-/-}$  cells (Figure S27B). Of note, RasGTP production is clearly impaired in moderately stimulated  $SOS1^{-/-}SOS2^{-/-}$  cells (Figure S27C). RasGTP levels in wildtype DT40 cells were sensitive to PP2 inhibition at the initiation of BCR stimulation. When cells were allowed to generate RasGTP for the first three minutes prior to PP2 addition, hysteresis was observed since RasGTP levels were high when compared to cases where the same dose of PP2 was added at the initiation of BCR stimulation (Figure 6E). In sharp contrast,  $SOS1^{-/-}SOS2^{-/-}$  cells do not exhibit hysteresis, and RasGTP levels decrease with increasing amounts of PP2 on the way up (PP2 at  $t=0$ ) and the way down (PP2 at  $t=3$ ) (Figure 6F).

### **Bistability and hysteresis provide Ras signaling memory during serial stimulation**

T cell activation may require integration of membrane-proximal signals from sequential contacts (each approximately 3 minutes in duration) that occur between T cells and antigen presenting cells in lymphoid tissues (Bouso and Robey, 2003; Henrickson et al., 2008; Skokos et al., 2007). A molecular mechanism that enables T cells to “remember” past encounters with antigen is not known.

Suppose during a T cell-APC contact the quality and quantity of encountered pMHC ligands is sufficient to stimulate engagement of the SOS feedback loop and robust Ras activation, but insufficient for other events necessary for T cell activation. The T cell disengages from the APC, and is not subject to stimulation until it encounters another APC. During this period the stimulus is “off”, and active Ras levels decline because phosphatases act on pLAT (Figure 2) causing SOS to disengage from the membrane, RasGAPs reduce RasGTP levels during the time that the stimulus is “off”, etc.. Suppose that during the next encounter of this T cell with an APC it encounters a weak stimulus that would not result in robust Ras activation if this T cell had not been previously robustly stimulated. We asked whether the existence of an underlying bistable steady-state structure due to feedback regulation of SOS (Figure 1) would result in restoration of robust Ras activation upon weaker re-stimulation. If so, bistability and hysteresis would be manifested as a molecular memory that enables integration of serially encountered weak signals after exposure to a strong stimulus.



To explore this idea, we carried out calculations with the minimal model shown in Figure 1. Robust stimulation of active Ras due to high levels of  $SOS_{cat}$  was followed by suddenly removing the stimulus. We then studied the dynamics of re-stimulation with a weak stimulus (green) after the originally strong stimulus has been “off” for a certain time (Figure 6G). Increasing the duration of the resting phase reduces the RasGTP level at the time of re-stimulation, because of the RasGAPs present in our model. Figure 6G shows that maximal activation is recovered upon re-stimulation with a subsequent weaker stimulus, provided that RasGTP does not decline below the level of the unstable steady state (blue points in Figure 1C). If RasGTP levels decline to baseline during the duration when the stimulus is “off”, then RasGTP levels are low upon re-stimulation (Figure 6G, 500 sec. rest period). If there is no bistability and hysteresis as when  $SOS_{cat}$  is not subject to feedback regulation (or Ras is activated via RasGRP), re-stimulation with a weak stimulus results in low levels of Ras activation regardless of prior stimulation; i.e., there is no memory (Figure 6H).

Stimulation of Jurkat T cells or B cells with the plant lectin Concanavalin A (Con A) results in robust calcium responses that rely on binding of ConA to the TCR or BCR (Weiss et al., 1987). Importantly, binding of Con A can be relatively rapidly abrogated by addition of  $\alpha$ -methyl-mannoside ( $\alpha$ -MM), a competitive carbohydrate. We used this protocol to test the predictions in Figure 6G and 6H. Because T and B cells respond similarly to this protocol, we used the DT40 system as it enables testing the effects of SOS by genetic deletion (Figure 6I).

ConA stimulation resulted in robust Ras activation in both wildtype and  $SOS1^{-/-}SOS2^{-/-}$  DT40 B cells at 3 minutes (Figure 6J). Addition of  $\alpha$ -MM treatment to robustly stimulated wildtype cells resulted in a decline in RasGTP levels. It is important to note that at 12 minutes, RasGTP levels still remained moderately above the basal level. Next, we tested the effect of a very weak stimulus of anti-BCR crosslinking antibody given at this 12-minute time point (see Figure 6K). Priming with ConA followed by  $\alpha$ -MM treatment resulted in hyperresponsive RasGTP levels induced by this weak second signal that did not elicit a response when wildtype DT40 B cells were primed with PBS as a negative control (Figure 6K). In contrast, when doubly-deficient  $SOS1^{-/-}SOS2^{-/-}$  DT40 B cells were primed through the same regimen, we observed only minimal RasGTP stimulation by the second signal mediated by the BCR (Figure 6L). These data are consistent with the prediction (Figure 6G and H) that the underlying bistability and hysteresis due to feedback regulation of SOS confers memory to the dynamic responses of previously stimulated lymphoid cells.

## DISCUSSION

### Major findings

We combined theoretical analyses and stochastic computer simulations to study membrane-proximal signaling in lymphocytes, with a view toward understanding how activation of a key signaling intermediate in diverse cell types (Ras) is regulated. Experimental tests of these predictions using diverse approaches, and further *in silico* and *in vitro* studies lead to the following conclusions. A feedback loop associated with SOS-mediated Ras activation is necessary for digital signaling in lymphoid cells, and hysteresis in the dose-response curve for Ras activation. Digital signaling and hysteresis may also confer lymphocytes with short-term molecular memory of encounters with antigen (Figure 7). Alone, RasGRP-mediated Ras activation results in analog signaling in cell lines and lymph node T cells and does not exhibit hysteresis. But, intermediate levels of RasGRP activity lead to more efficient digital responses than with SOS alone. The interplay of differential activities of these two RasGEFs leading to efficient and varied cellular responses may be a principle that is employed more broadly and could have important implications for lymphocyte function. Our *in silico* and *in vitro* studies predict many phenomena that should be explored further.

### Further experimental tests of predicted Ras signaling characteristics

We have demonstrated that digital Ras-ERK signaling requires SOS in cells lines (Figure 5). Similar TCR-induced digital signals operate in primary T cells, but currently a direct demonstration of the involvement of SOS' positive feedback loop in primary cells is lacking. Future work to address this point will be aided by the generation of the appropriate mouse models.

Compartmentalized Ras signaling has received considerable recent interest (Campbell et al., 1998; Mor and Philips, 2006). SOS activates Ras exclusively at the plasma membrane, but RasGRP can also function on internal membranes. It will of interest to investigate how analog (RasGRP) and digital (SOS) mechanisms of Ras activation occur in time and space as well as whether recently observed spatial nano-clustering of active Ras proteins (Tian et al., 2007) is influenced by positive feedback regulation of Ras activation.

In other cell types digital signaling has been reported to rely on a positive feedback loop between MAPK and phospholipase A<sub>2</sub> (Bhalla and Iyengar, 1999). Phospholipase A<sub>2</sub> is, however, not expressed in T and B lymphocytes (Gilbert et al., 1996). This may be why digital signaling in lymphocytes is controlled by feedback regulation of SOS' GEF activity. Nonetheless, feedback loops present in the MAPK pathway (Ferrell, 2002; Kholodenko et al., 2002) undoubtedly further modulate our measurements of CD69 and ERK activation, and it will be important to examine how. Such investigations could help resolve puzzles such as why in SOS1<sup>-/-</sup>SOS2<sup>-/-</sup> cells RasGTP levels are lower when PP2 is added after robust stimulation compared to when the inhibitor is added at t=0, or why wildtype Jurkat and DT40 cells exhibit more pronounced hysteresis for higher doses of PP2 (Figure 6). These studies may also resolve whether delayed action of nuclear phosphatases that turn off ERK cause apparent hysteresis in ERK activation in SOS<sup>-/-</sup> DT40 cells without bistability (Figure S28).

### Predicted functional implications of digital signaling and hysteresis

The sharp threshold in the dose-response curve (i.e., digital signaling) originating from feedback regulation of SOS' GEF activity may provide an additional membrane-proximal checkpoint that prevents spurious T cell activation. Weak receptor stimulation could lead to low levels of TCR and ZAP-70 activation that do not efficiently recruit SOS to the membrane or produce sufficiently large levels of RasGTP via the RasGRP pathway. Thus, the SOS feedback loop will not ignite (Figure 7A), and the resulting low levels of downstream signaling will prevent spurious T cell activation in response to weak stimulation. In contrast, when receptor stimulation exceeds a threshold, the SOS feedback loop will be engaged resulting in a sharp/digital increase in downstream signaling. It has been suggested that digital ERK signaling, along with feedback regulation of Lck, may enable discrimination between ligands of varying potency (Altan-Bonnet and Germain, 2005).

If early signaling events do result in robust Ras activation, it would be undesirable to shut down signaling due to fluctuations in receptor-ligand binding. Hysteresis in the dose-response curve may stabilize signaling once it has proceeded past this checkpoint. We predict hysteresis to be observed for a finite time interval and for stimulus levels that are not far below the threshold. This may ensure that if the signal is absent for a sufficiently long time or falls below a threshold, signaling is terminated.

*In vivo* infections result in very low numbers of cognate peptide-MHC complexes on most APCs in lymphoid tissues. Recent studies have suggested that T cell activation in such circumstances requires integration of interrupted serial encounters with APCs bearing cognate ligands (Henrickson et al, 2008). Our results suggest that, if a T cell's membrane-proximal signaling machinery is robustly stimulated once, the short-term molecular memory conferred

by feedback regulation of SOS (Figure 6) could enable subsequent weaker signals to robustly stimulate these cells, thereby enabling signal integration. This concept could be examined by combining intravital microscopy with imaging of signaling products such as Ras to test whether hysteresis during Ras activation plays a role in signal integration *in vivo*.

The threshold potency above which strongly binding ligands negatively select thymocytes in the thymus is very sharp while the positive selection threshold is graded (Daniels et al., 2006). This may be because negative selection results from strong signaling requiring active Ras levels that can be realized only upon ignition of the SOS feedback loop. The resulting digital response may correspond to the sharp boundary separating ligands that induce positive and negative selection in the thymus. Weak stimulation may only activate Ras via the RasGRP pathway, thereby eliciting purely analog responses during positive selection. This potential ability of RasGRP and SOS acting to mediate either analog or digital signaling which impacts T cell development needs to be further examined in mouse models developed with the aim of impairing analog or digital signaling.

## Experimental Procedures

### Mean-field equations for the minimal model shown in Figure 1

The minimal model is based on the following reactions shown in Figure 1A. The mass action rate equations corresponding to those reactions are,

$$\frac{d[S]}{dt} = -k_1[S][R_D] + k_{-1}[SR_D] - k_2[S][R_T] + k_{-2}[SR_T] \quad (1a)$$

$$\frac{d[SR_T]}{dt} = k_2[S][R_T] - k_{-2}[SR_T] \quad (1b)$$

$$\frac{d[R_T]}{dt} = -k_2[S][R_T] + k_{-2}[SR_T] + \frac{k_3^{cat}[R_D][SR_T]}{K_{3m} + [R_D]} + \frac{k_4^{cat}[R_D][SR_D]}{K_{4m} + [R_D]} - \frac{k_5^{cat}[R_{GAP}][R_T]}{K_{5m} + [R_T]} \quad (1c)$$

The total number of SOS and Ras molecules are conserved which leads to the following constraints:

$$\alpha = [S] + [SR_D] + [SR_T]$$

$$\beta = [R_D] + [R_T] + [SR_D] + [SR_T]$$

In the above equations, [X] represents the concentration of the species, X. The abbreviations used for different species are:

$$S \equiv \text{SOS} \quad R_D \equiv \text{Ras} - \text{GDP} \quad R_T \equiv \text{Ras} - \text{GTP}$$

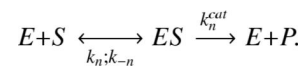
$$SR_D \equiv \text{SOS} - \text{Ras} - \text{GDP} \quad SR_T \equiv \text{SOS} - \text{Ras} - \text{GTP}$$

$$R_{GAP} \equiv \text{Ras} - \text{GAP}$$

The Michealis constants are defined as,

$$K_{3m} = (k_3^{cat} + k_{-3})/k_3; K_{4m} = (k_4^{cat} + k_{-4})/k_4; K_{5m} = (k_5^{cat} + k_{-5})/k_5, \text{ where, } k_n, k_{-n} \text{ are the binding,}$$

unbinding rates of the substrate (S) to the enzyme (E), respectively, and  $k_n^{cat}$  is the rate of production of the product (P) from the complex (ES). The reaction is shown schematically below:



$K_{3m}$ ,  $K_{4m}$  and  $K_{5m}$  are calculated from Table S1. For the ODE in Eq.(1), reactions, #1 and #2 in Table S1, for Eq.(2), reaction, #2 in Table S1, and for Eq.(3), reactions, #2, #3, #4 and #5 are used. For the reactions in #3, #4 and #5 in Table S1, we used the Michaelis Menten form, and the Michaelis constants are calculated from the binding, unbinding and the catalytic rates of the reactions as described above. In many cases, the  $K_D(=k_{off}/k_{on})$  values are known for the reactions but the binding ( $k_{on}$ ) and unbinding ( $k_{off}$ ) rates are not known. Therefore, we carried out parameter sensitivity analyses, and our results are robust to up to 10-fold variations of the parameters. The details of this analysis are shown in Table S3. The left hand sides of Eqs. 1a–c are set to zero and the algebraic equations are solved for the steady-state concentrations.

### Stochastic simulations of the model shown in Figures 2 and 4

We performed stochastic simulations which effectively solve the Master equation (Kampen, 1992) corresponding to the chemical reactions in the signaling network shown in Figure 2a using the Gillespie algorithm (Bortz B, 1975; Gillespie, 1977; McAdams and Arkin, 1997). Simulation details and rather exhaustive parameter sensitivity analyses are provided in the supplement (Sections II and III).

### Cell biological procedures

All cell biological procedures are described in the supplement, Section IV, pages 67–72.

### Supplementary Material

Refer to Web version on PubMed Central for supplementary material.

### Acknowledgements

We thank Dr. Kurosaki for DT40 lines and Dr. Dafna Bar-sagi for the H-RasG59E38 plasmid. We are grateful to Dr. DeFranco and members of the Weiss, Chakraborty, and Roose labs for critically reading of the manuscript. We apologize to colleagues we could not cite due to space constraints. Financial support: NIH Director's Pioneer Award and IPO1 (AKC), the Howard Hughes Medical Institute as well as the Rosalind Russell Medical Research Center for Arthritis (AW), and the Sandler Foundation (JR).

### References

- Altan-Bonnet G, Germain RN. Modeling T cell antigen discrimination based on feedback control of digital ERK responses. *PLoS Biol* 2005;3:e356. [PubMed: 16231973]
- Barkai N, Leibler S. Circadian clocks limited by noise. *Nature* 2000;403:267–268. [PubMed: 10659837]
- Bhalla US, Iyengar R. Emergent properties of networks of biological signaling pathways. *Science* 1999;283:381–387. [PubMed: 9888852]
- Bortz BKM, Lebowitz JL. *Journal of Computational Physics* 1975;17
- Bouso P, Robey E. Dynamics of CD8(+) T cell priming by dendritic cells in intact lymph nodes. *Nature immunology* 2003;4:579–585. [PubMed: 12730692]
- Boykevisch S, Zhao C, Sondermann H, Philippidou P, Halegoua S, Kuriyan J, Bar-Sagi D. Regulation of ras signaling dynamics by Sos-mediated positive feedback. *Curr Biol* 2006;16:2173–2179. [PubMed: 17084704]

- Campbell SL, Khosravi-Far R, Rossman KL, Clark GJ, Der CJ. Increasing complexity of Ras signaling. *Oncogene* 1998;17:1395–1413. [PubMed: 9779987]
- Corbalan-Garcia S, Margarit SM, Galron D, Yang SS, Bar-Sagi D. Regulation of Sos activity by intramolecular interactions. *Mol Cell Biol* 1998;18:880–886. [PubMed: 9447984]
- Daniels MA, Teixeira E, Gill J, Hausmann B, Roubaty D, Holmberg K, Werlen G, Hollander GA, Gascoigne NR, Palmer E. Thymic selection threshold defined by compartmentalization of Ras/MAPK signalling. *Nature* 2006;444:724–729. [PubMed: 17086201]
- Dower NA, Stang SL, Bottorff DA, Ebinu JO, Dickie P, Ostergaard HL, Stone JC. RasGRP is essential for mouse thymocyte differentiation and TCR signaling. *Nature immunology* 2000;1:317–321. [PubMed: 11017103]
- Ebinu JO, Stang SL, Teixeira C, Bottorff DA, Hooton J, Blumberg PM, Barry M, Bleakley RC, Ostergaard HL, Stone JC. RasGRP links T-cell receptor signaling to Ras. *Blood* 2000;95:3199–3203. [PubMed: 10807788]
- Elf J, Ehrenberg M. Spontaneous separation of bi-stable biochemical systems into spatial domains of opposite phases. *Syst Biol (Stevenage)* 2004;1:230–236. [PubMed: 17051695]
- Ferrell JE. Self-perpetuating states in signal transduction: positive feedback, double-negative feedback and bistability. *Current Opinion in Cell Biology* 2002;14:140–148. [PubMed: 11891111]
- Freedman TS, Sondermann H, Friedland GD, Kortemme T, Bar-Sagi D, Marqusee S, Kuriyan J. A Ras-induced conformational switch in the Ras activator Son of sevenless. *Proc Natl Acad Sci U S A* 2006;103:16692–16697. [PubMed: 17075039]
- Genot E, Cantrell DA. Ras regulation and function in lymphocytes. *Curr Opin Immunol* 2000;12:289–294. [PubMed: 10781411]
- Gilbert JJ, Stewart A, Courtney CA, Fleming MC, Reid P, Jackson CG, Wise A, Wakelam MJ, Harnett MM. Antigen receptors on immature, but not mature, B and T cells are coupled to cytosolic phospholipase A2 activation: expression and activation of cytosolic phospholipase A2 correlate with lymphocyte maturation. *J Immunol* 1996;156:2054–2061. [PubMed: 8690892]
- Gillespie DT. Exact Stochastic Simulation of Coupled Chemical-Reactions. *Journal of Physical Chemistry* 1977;81:2340–2361.
- Hartigan JA, Hartigan PM. The Dip Test of Unimodality. *Annals of Statistics* 1985:15.
- Henrickson SE, Mempel TR, Mazo IB, Liu B, Artyomov MN, Zheng H, Peixoto A, Flynn MP, Senman B, Junt T, et al. T cell sensing of antigen dose governs interactive behavior with dendritic cells and sets a threshold for T cell activation. *Nature immunology* 2008;9:282–291. [PubMed: 18204450]
- Houtman JC, Yamaguchi H, Barda-Saad M, Braiman A, Bowden B, Appella E, Schuck P, Samelson LE. Oligomerization of signaling complexes by the multipoint binding of GRB2 to both LAT and SOS1. *Nature structural & molecular biology* 2006;13:798–805.
- Kampen, NGv. Rev and enl edn. Amsterdam; New York, North-Holland: 1992. Stochastic processes in physics and chemistry.
- Kholodenko BN, Kiyatkin A, Bruggeman FJ, Sontag E, Westerhoff HV, Hoek JB. Untangling the wires: a strategy to trace functional interactions in signaling and gene networks. *Proc Natl Acad Sci U S A* 2002;99:12841–12846. [PubMed: 12242336]
- Margarit SM, Sondermann H, Hall BE, Nagar B, Hoelz A, Pirruccello M, Bar-Sagi D, Kuriyan J. Structural evidence for feedback activation by Ras.GTP of the Ras-specific nucleotide exchange factor SOS. *Cell* 2003;112:685–695. [PubMed: 12628188]
- McAdams HH, Arkin A. Stochastic mechanisms in gene expression. *Proc Natl Acad Sci U S A* 1997;94:814–819. [PubMed: 9023339]
- Mor A, Philips MR. Compartmentalized Ras/MAPK signaling. *Annu Rev Immunol* 2006;24:771–800. [PubMed: 16551266]
- Prasad A, Zikherman J, Das J, Roose JP, Weiss A, Chakraborty AK. Origin of the sharp boundary that discriminates positive and negative selection of thymocytes. *PNAS*. in press
- Roose JP, Mollenauer M, Gupta VA, Stone J, Weiss A. A Diacylglycerol-Protein Kinase C-RasGRP1 Pathway Directs Ras Activation upon Antigen Receptor Stimulation of T Cells. *Mol Cell Biol* 2005;25:4426–4441. [PubMed: 15899849]

- Roose JP, Mollenauer M, Ho M, Kurosaki T, Weiss A. Unusual interplay of two types of Ras activators, RasGRP and SOS, establishes sensitive and robust Ras activation in lymphocytes. *Mol Cell Biol* 2007;27:2732–2745. [PubMed: 17283063]
- Ruiz S, Santos E, Bustelo XR. RasGRF2, a guanosine nucleotide exchange factor for Ras GTPases, participates in T-cell signaling responses. *Mol Cell Biol* 2007;27:8127–8142. [PubMed: 17923690]
- Skokos D, Shakhar G, Varma R, Waite JC, Cameron TO, Lindquist RL, Schwickert T, Nussenzweig MC, Dustin ML. Peptide-MHC potency governs dynamic interactions between T cells and dendritic cells in lymph nodes. *Nature immunology* 2007;8:835–844. [PubMed: 17632517]
- Sondermann H, Soisson SM, Boykevich S, Yang SS, Bar-Sagi D, Kuriyan J. Structural analysis of autoinhibition in the Ras activator Son of sevenless. *Cell* 2004;119:393–405. [PubMed: 15507210]
- Starr TK, Jameson SC, Hogquist KA. Positive and negative selection of T cells. *Annu Rev Immunol* 2003;21:139–176. [PubMed: 12414722]
- Tian T, Harding A, Inder K, Plowman S, Parton RG, Hancock JF. Plasma membrane nanoswitches generate high-fidelity Ras signal transduction. *Nat Cell Biol* 2007;9:905–914. [PubMed: 17618274]
- Wang DZ, Hammond VE, Abud HE, Bertoncillo I, McAvoy JW, Bowtell DD. Mutation in Sos1 dominantly enhances a weak allele of the EGFR, demonstrating a requirement for Sos1 in EGFR signaling and development. *Genes Dev* 1997;11:309–320. [PubMed: 9030684]
- Weiss A, Shields R, Newton M, Manger B, Imboden J. Ligand-receptor interactions required for commitment to the activation of the interleukin 2 gene. *J Immunol* 1987;138:2169–2176. [PubMed: 3104454]

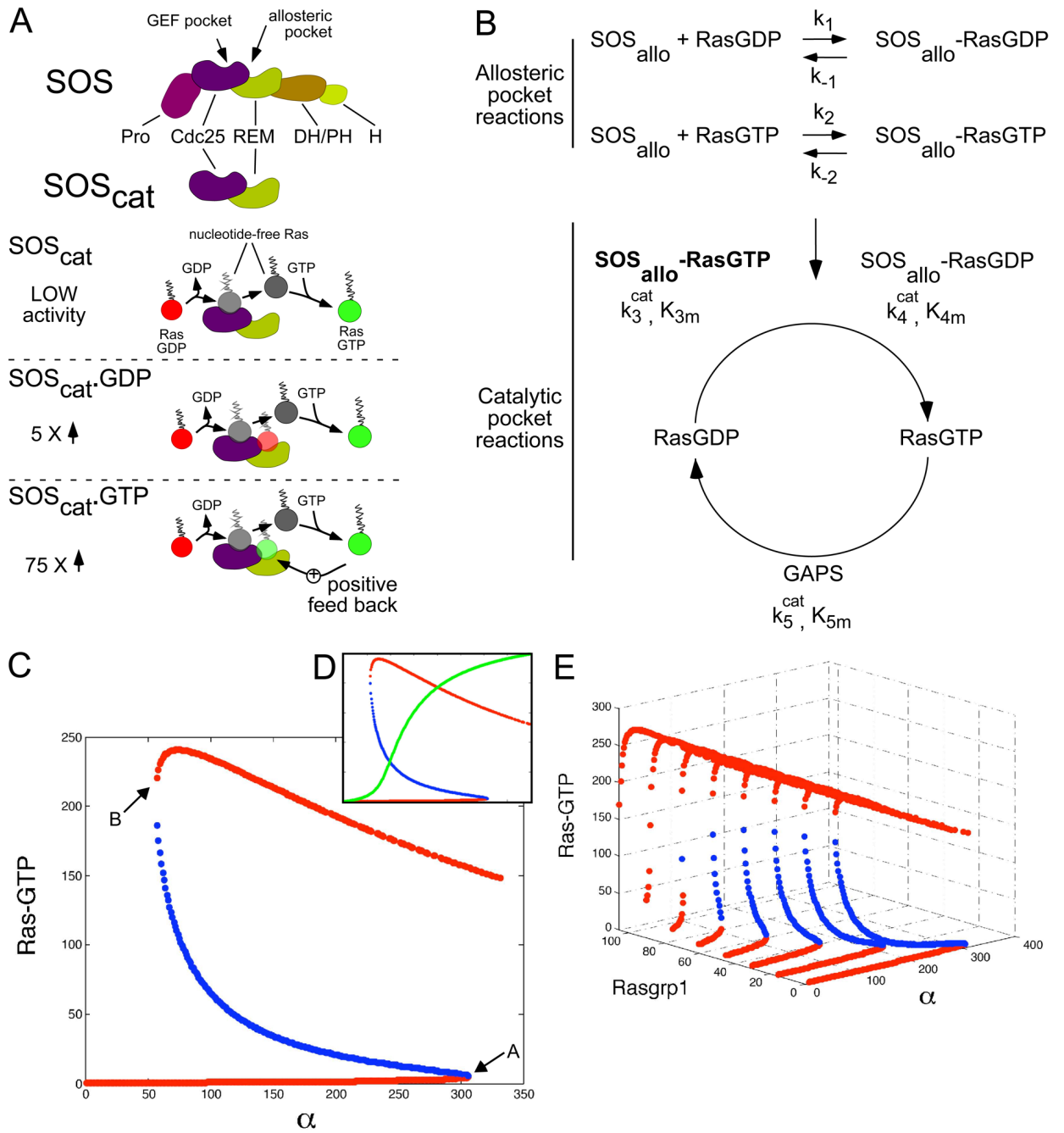


**Figure 1. A minimal model of the catalytic domain of SOS predicts three possible states of Ras activation**

(A) SOS' protein domains, GEF pocket, and allosteric pocket. Pro = proline-rich, Cdc25 = Cdc25 homology domain, REM = Ras exchange motif, DH/PH = Dbl-homology, Pleckstrin-homology domain, H = Histone folds. SOS<sub>cat</sub> includes the catalytic region which contains both the GEF and the allosteric pockets. Illustration of SOS<sub>cat</sub>'s mode of Ras activation. Note that binding of RasGTP to the allosteric pocket increases SOS<sub>cat</sub>'s activity 75 fold, establishing a positive feedback loop.

(B) Depiction of the allosteric pocket and catalytic site reactions on SOS<sub>cat</sub>. SOS<sub>allo</sub>-Ras-GTP in bold reflects the 75 fold increased catalytic activity.

(C) Steady states of the mean-field kinetic rate equations show production of low and high concentrations of RasGTP (characterized by stable fixed points in red) at low and high values of  $\alpha$ .  $\alpha$  represents the total number of  $\text{SOS}_{\text{cat}}$  molecules in the simulation box (see Supplement, Section I). At intermediate levels of  $\alpha$ , three states arise with unstable fixed Ras-GTP points shown in blue.

(D) Overlay with analysis in 1C. The green line represents simulations when the allosteric pocket of  $\text{SOS}_{\text{cat}}$  is mutated in a way that it cannot bind to Ras-GDP or Ras-GTP. In order to demonstrate the overlay in the same graph, the low catalytic rate ( $k_{\text{cat}} \sim 0.0005 \text{ s}^{-1}$ ) of the mutant  $\text{SOS}_{\text{cat}}$  was artificially increased to  $0.038 \text{ s}^{-1}$ .

(E) Steady state activation of Ras-GTP as a function of  $\text{SOS}_{\text{cat}}$  and RasGRP. The RasGRP-DAG complex (abbreviated RasGRP) catalyzes Ras-GDP following the reactions shown in reaction #8 in Table S4. This reaction is incorporated in the ODE model:

$k_8^f [\text{RasGRP} - \text{DAG}] [\text{Ras} - \text{GDP}] / (K_{8m} + [\text{Ras} - \text{GDP}])$ , in Eq.(1c) with  $k_8^f = 0.01 \text{ s}^{-1}$  and  $K_{8m} = 3.06 \mu\text{M}$ , calculated from Table S4. Unstable and stable points are shown in blue and red respectively.



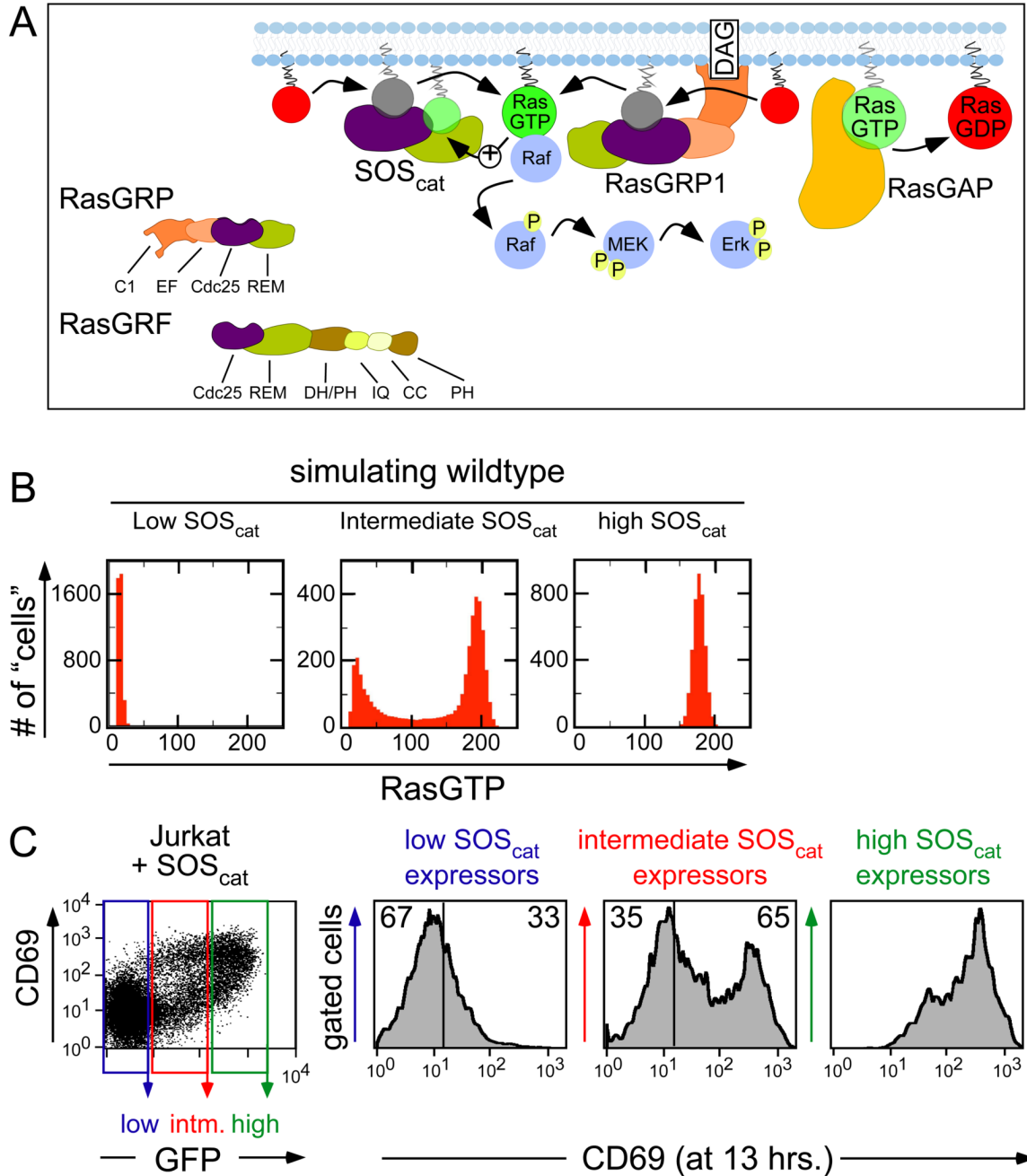


**Figure 2. Bimodal Ras activation induced by  $SOS_{cat}$  operating in the Ras signaling network occurs in a stochastic model and in a T cell line**

(A) Representation of  $SOS_{cat}$  function in the context of the Ras signaling network. Besides  $SOS$ -1 and -2, lymphocytes express the RasGEFs RasGRP-1 and -3 and RasGRF2. C1 = DAG-binding C1 domain, EF = calcium-binding EF hand. IQ = motif for calcium/calmodulin binding, CC = coiled coil. RasGTP produced by RasGRP1 can influence  $SOS$ ' activity via the allosteric pocket. Of note, deficiency of RasGRF2 does not appear to impact T cell Ras activation but influences the calcium-NFAT pathway (Ruiz et al., 2007).

(B) Distributions of RasGTP calculated from our stochastic simulation algorithm at low, intermediate, or high levels of  $SOS_{cat}$  (2 fold increments) in a wild type "cell". At intermediate

levels of  $SOS_{cat}$  a bimodal RasGTP pattern arises. See Section II (Tables S4-S8, Figures S5-S12) for additional information.

(C) Introduction of intermediate levels of  $SOS1_{cat}$  into a wildtype Jurkat T cell line leads to bimodal upregulation of CD69. Cells were cotransfected with ten  $\mu\text{g}$  of GFP- and ten  $\mu\text{g}$  of  $SOS1_{cat}$ -expressing plasmid. The dot plot depicts CD69 and GFP expression on individual cells, analyzed by FACS. Electronic gates define low, medium, and high GFP expression, reflecting low, medium, and high expression of the co-transfected  $SOS1_{cat}$  plasmid. CD69 expression was analyzed in histograms for the three different gates. See Figure S21B for protein expression levels. 2C is a representative example of three independent experiments.

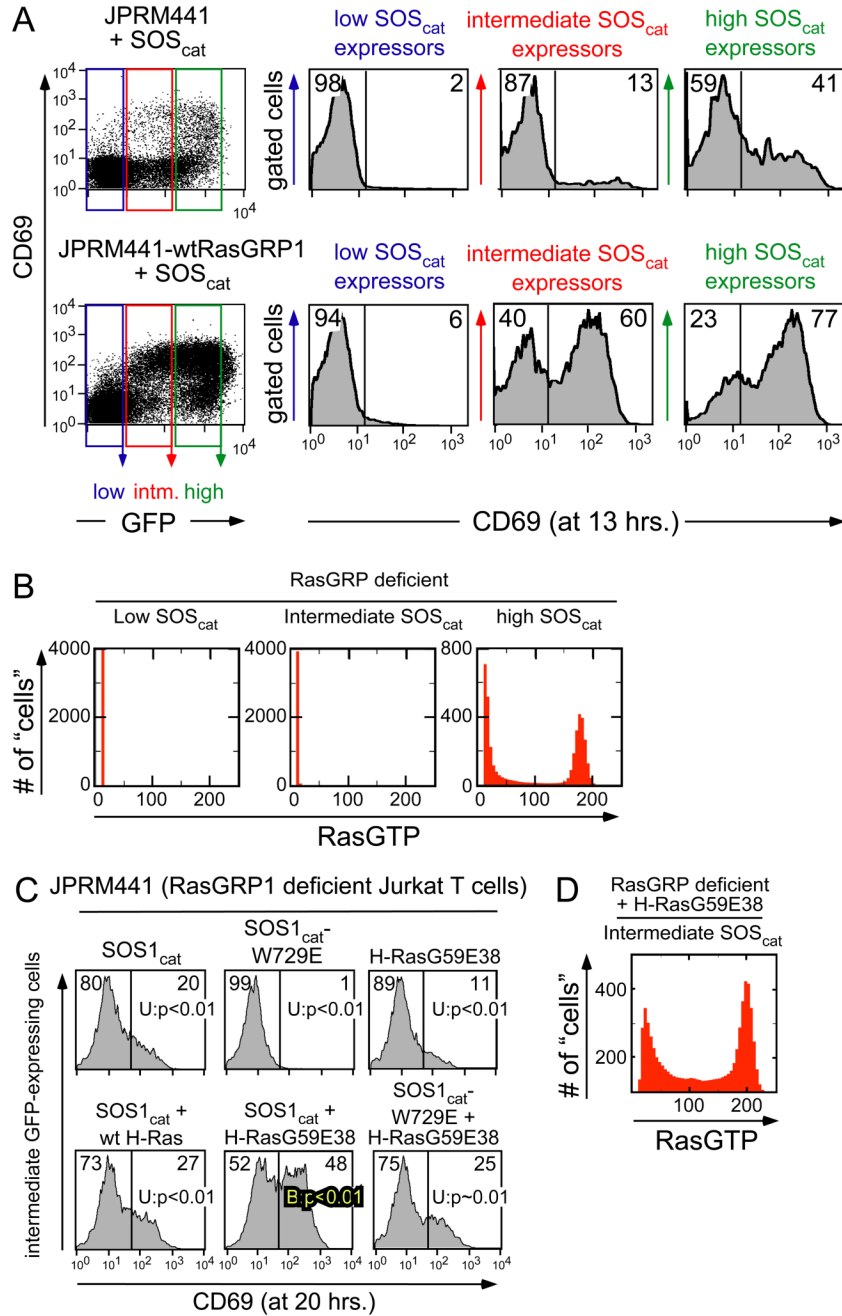


**Figure 3. A RasGTP mimetic restores efficient  $SOS_{cat}$ -induced bimodal signals in RasGRP deficient cells**

(A) Analysis of the efficiency of  $SOS_{cat}$ -induced Ras signaling in a RasGRP1-deficient Jurkat T cell line (JPRM441) and its wildtype RasGRP1-reconstituted derivative line (JPRM441-wtRasGRP1). Experimentation and analysis as in figure 2C, see also Figure S21B. Intermediate  $SOS_{cat}$  induces high levels of CD69 expression in only 13% of the JPRM441 cells. This relative defect in JPRM441 cells is restored to 60% in the JPRM441-wtRasGRP1 cells.

(B) Stochastic simulations as in 2B. Histograms of Ras-GTP simulating a RasGRP deficient state are depicted. Increments of  $SOS_{cat}$  between the plots are 2 fold. Note the lack of a bimodal distribution in "cells" with intermediate  $SOS_{cat}$ .

(C) Introduction of a RasGTP mimetic overcomes RasGRP1 deficiency in JPRM441 cells. JPRM441 cells were transfected with GFP together with  $SOS_{cat}$ ,  $SOS_{cat} -W729E$  (allosteric pocket mutant), H-RasG59E38 (RasGTP mimetic), H-Ras, or combinations thereof. CD69 expression was analyzed by FACS and depicted as histograms for the intermediate GFP-expressing cells. Histograms were subsequently analyzed by a Hartigan's statistical test to examine uni- versus bi-modality. See figure S24. H-RasG59E38 synergizes with  $SOS_{cat}$  to produce a bimodal pattern (Hartigan's test;  $B;p<0.01$ ), but not with  $SOS_{cat} -W729E$ . For detailed description and expression levels of introduced proteins see figure S23. Figure 3C is representative of results in three independent experiments.

(D) Stochastic simulations introducing a H-RasG59E38 molecule into the mathematical model. Note the reappearance of a bimodal response in "cells" with intermediate  $SOS_{cat..}$ , compared to Figure 3B.

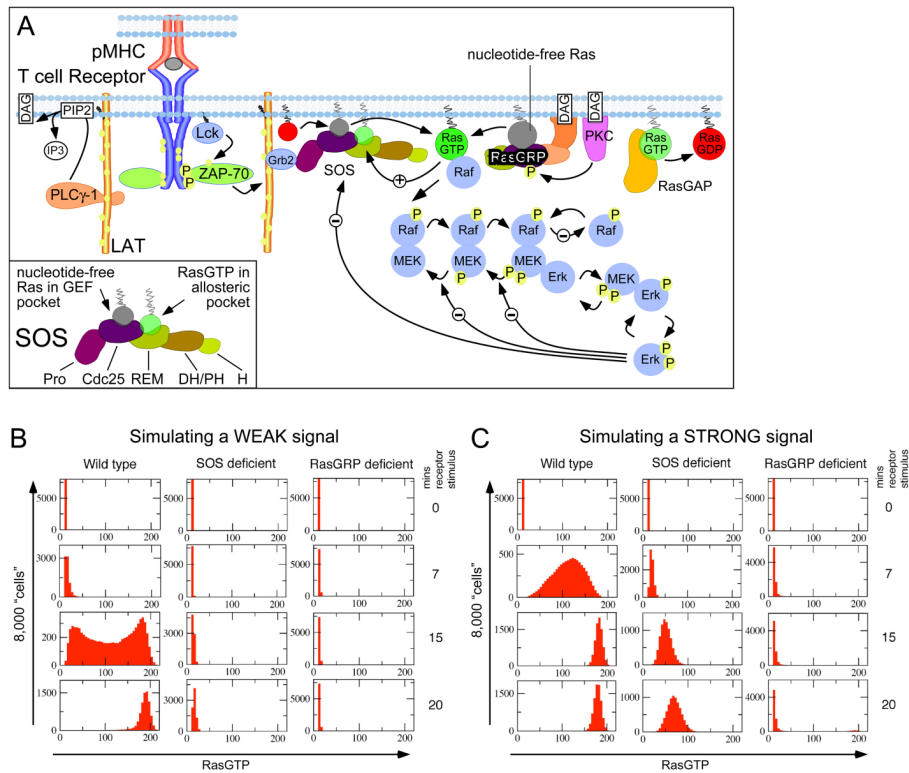


**Figure 4. Digital antigen receptor induced Ras activation *in silico***

(A) Representation of the Ras signaling network in T lymphocytes that is simulated by our stochastic simulation algorithm. Lck phosphorylates TCR $\zeta$  leading to recruitment of ZAP-70. ZAP-70 phosphorylates LAT resulting in the recruitment of Grb2-SOS and PLC $\gamma$ 1. DAG produced by PLC $\gamma$ 1 leads to phosphorylation of RasGRP1 by PKC $\theta$ . Both SOS and RasGRP1 produce RasGTP signaling downstream to RAF, MEK, and ERK. B lymphocytes express PLC $\gamma$ 2 and downstream signaling events are very similar to those in T lymphocytes.

(B) Ras activation in 8,000 “cells” in simulation induced by weak receptor signals over time. A bimodal RasGTP pattern emerges in wildtype, but not SOS or RasGRP deficient states. (C) Same as in (B) but simulating strong receptor signals. RasGTP levels rapidly increase in the wildtype “cells”. A graded increase in RasGTP is observed in the SOS deficient system. See supplement, Section III (Tables S9–S13, Figures S13–S20) for additional information, parameters, and parameter variation tests.

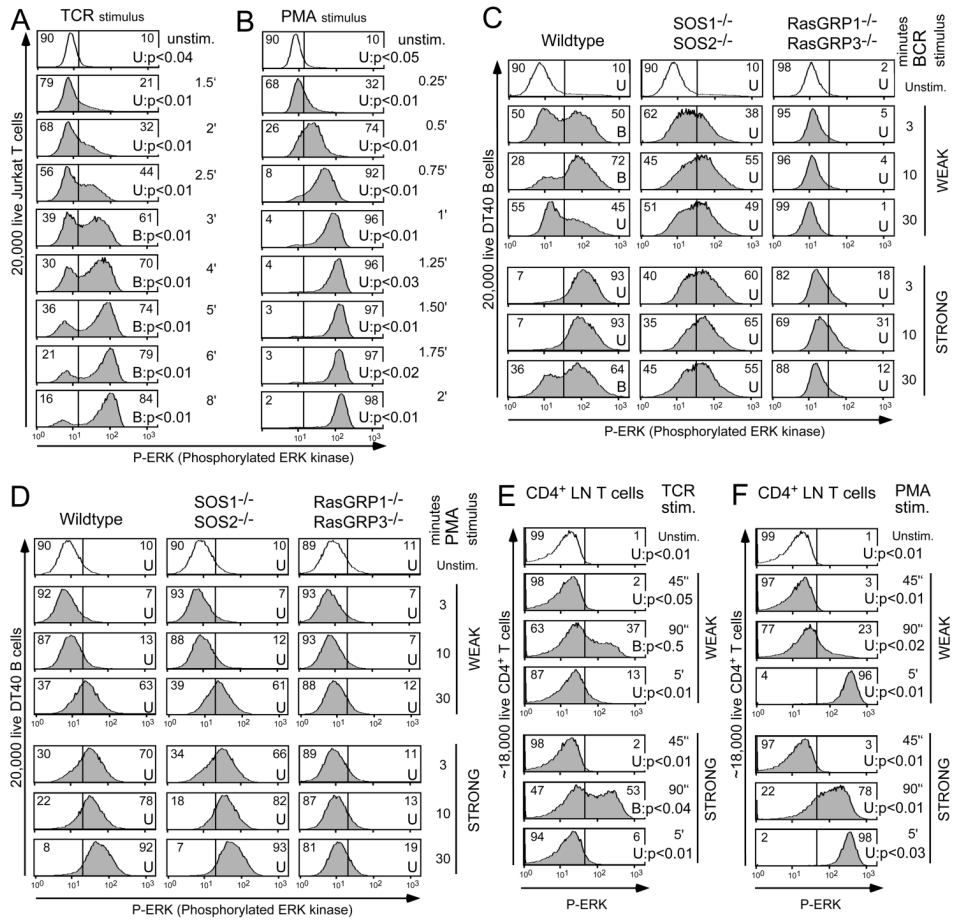


**Figure 5. RasGRP induces analog phospho-ERK signals, whilst SOS induces digital signals in B cell lines and primary T cells**

(A) Fluorescence flow cytometric analysis of ERK phosphorylation in 20,000 individual Jurkat T cells per histogram. Cells were stimulated for the indicated time intervals with a TCR stimulating antibody (1:500 dilution of C305). ERK phosphorylation initially occurs in a unimodal fashion and switches to a bimodal pattern (Hartigan’s tests). Numbers inside the histograms represent the percentage of cells on either side of the divider.

(B) As in (A) but cells were stimulated with 25 ng/ml PMA (a DAG analog) for shorter time intervals. Note the gradual increase of phospho-ERK over time without bimodal patterns.

(C) The indicated DT40 B cell lines were weakly or strongly stimulated through their BCR for 3, 10, or 30 minutes, or left unstimulated. “U” or “B” labels indicate unimodal or bimodal (Hartigan test). See figure S24 for methods, additional data and p-values.

(D) Same as in (C), except cells were stimulated with PMA; either weak (10 ng/ml) or strong (60 ng/ml). See figure S25 for additional data.

(E, F) Digital, TCR-induced, ERK phosphorylation in CD4 positive lymph node T cells, but analog PMA-induced ERK phosphorylation. Cells were stimulated by crosslinking their TCR in (E) or by PMA in (F). Figures 5A-F are representative examples of 2, 3, 3, 2, 3, and 2 independent experiments, respectively.

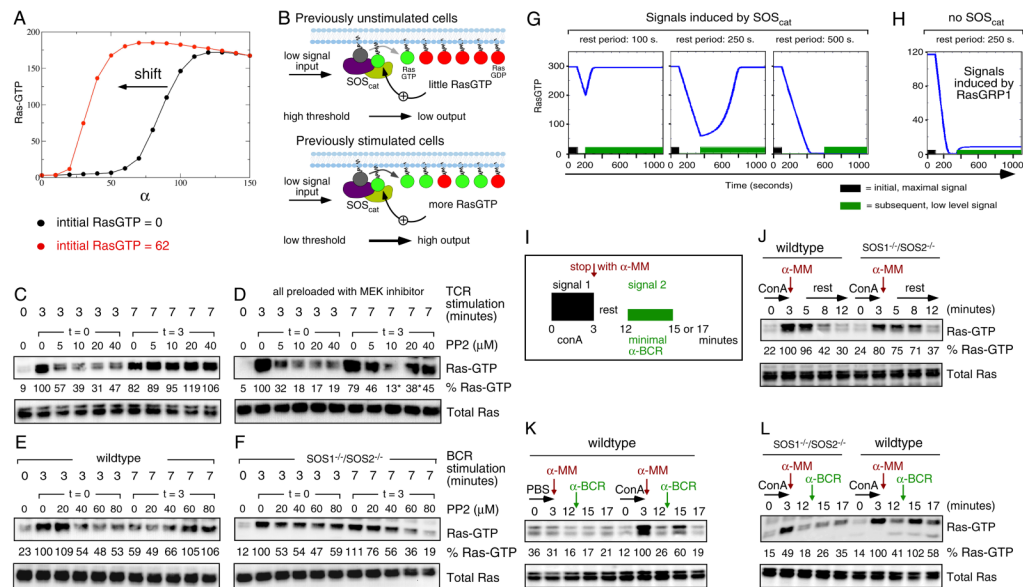


**Figure 6. Hysteresis at the level of RasGTP depends on SOS**

(A) Prediction of hysteresis in Ras activation from our stochastic simulation. Points in black and red denote Ras activations at a time  $t=10$  minutes when the cells had either 0 or 62 molecules/ $(\mu\text{m})^2$  of Ras-GTP concentrations at  $t=0$  minutes, respectively. All the simulations are done with a fixed RasGRP1 concentration at 500 molecules/ $(\mu\text{m})^3$ .

(B) Cartoon illustrating about the biochemical origin of hysteresis: a low level of remaining RasGTP that can bind the allosteric pocket in SOS.

(C–F) Analysis of GTP loaded Ras using pull-down assays. Lanes 3–6: cells stimulated for 3 minutes in the presence of increasing amounts of PP2 (Src kinase inhibitor) added simultaneously with the stimulus at  $t=0$ . Alternatively (lanes 8–11), cells were stimulated for 3 minutes, inhibitor was introduced at  $t=3$  minutes, and responses were analyzed at 7 minutes. Lane 1 is unstimulated, lanes 2 and 7 have no inhibitor added. Legend of the panels: (C) Jurkat T cells and (D) Jurkat T cells preloaded with U0126 MEK1/2 inhibitor both stimulated with 1:500 diluted C305 ( $\alpha$ -TCR), (E) wildtype DT40 B cells and (F)  $\text{SOS1}^{-/-}\text{SOS2}^{-/-}$  doubly deficient DT40 B cells both stimulated with 1:300 diluted M4 ( $\alpha$ -BCR). Experiments presented in 6C–F are representative examples of 3, 4, 5, and 3 independent experiments, respectively. Numbers indicate pixel intensity of the corresponding RasGTP, corrected for total Ras, one condition arbitrarily set at 100%. Due to a suboptimal blot transfer in 6D, 13%\* and 38%\* are under-representations of the level of generated RasGTP.

(G) Modeling serial stimulation. RasGTP (blue line) was initially induced by high levels of  $\text{SOS}_{\text{cat}}$  (black box, 350 molecules  $\alpha$ ).  $\text{SOS}_{\text{cat}}$  was removed for 100, 250, or 500 seconds and subsequent low level  $\text{SOS}_{\text{cat}}$  signals were simulated (green box, 150 molecules  $\alpha$ ). Provided that RasGTP levels do not fall below the blue points (Figure 1C), robust re-stimulation is induced by low level  $\text{SOS}_{\text{cat}}$ . The results are obtained from mean field rate equations corresponding to the pathway in Fig 1B and the parameters in Table 1.

(H) Lack of sensitized re-stimulation in the absence of SOS. The model from figure 1E is used to analyze a SOS deficient state in the same manner as Fig. 6G. RasGRP1 values were set at 100 (black) and 50 (green) molecules of RasGRP1 in the simulation box, respectively. The response to the second stimulus is history-independent.

(I) Experimental design to mimic serial stimulation of lymphocytes.

(J) Concanavilin A (ConA) induces RasGTP in wildtype DT40 and  $\text{SOS1}^{-/-}\text{SOS2}^{-/-}$  deficient DT40 B cells.  $\alpha$ -methyl mannoside ( $\alpha$ -MM) is added at  $t=3$  minutes to stop the ConA-induced

BCR stimulus (Weiss et al., 1987) and RasGTP levels decrease to slightly above basal levels at t=12 minutes.

(K) Previous RasGTP induction by ConA stimulation of wildtype DT40 B cells followed by  $\alpha$ -MM results in very sensitive induction of RasGTP by a second minimal BCR stimulus (1:4,500 diluted M4; 1/15<sup>th</sup> of the amount in 6E and F), whereas priming with PBS as negative control does not.

(L) Induction of RasGTP by ConA in  $SOS1^{-/-}SOS2^{-/-}$  deficient DT40 B cells does not result in sensitive RasGTP generation by a second signal (1:3,000 diluted M4;  $\alpha$ -BCR). Experiments presented in 6J-L are representative examples of 3, 4, and 2 independent experiments, respectively



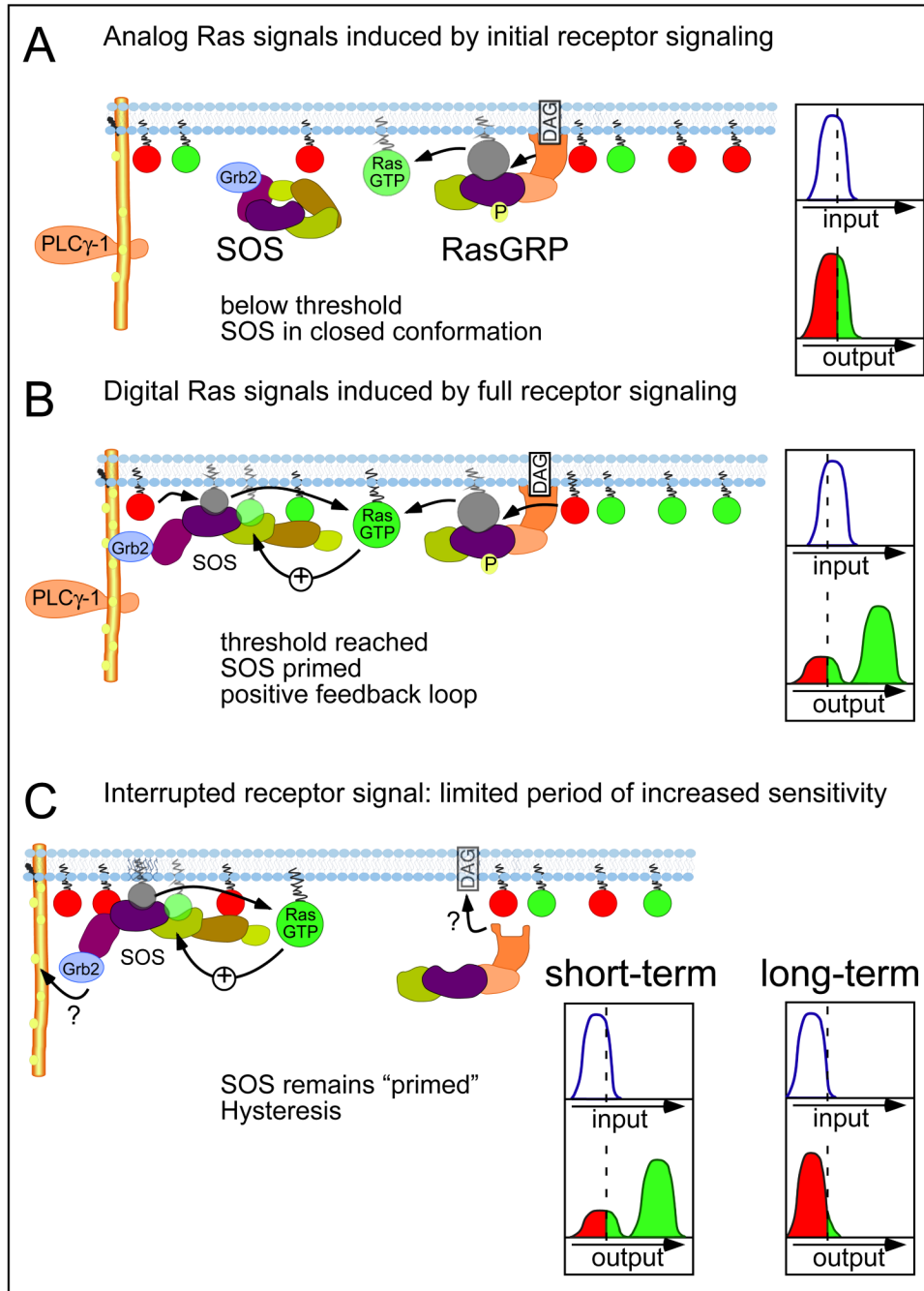


**Figure 7. Model of analog and digital signaling and hysteresis in lymphocytes**

(A) Upon initial receptor activation analog Ras signals are generated in lymphocytes because Ras activation occurs solely via RasGRP. Inset: a small graded increase in signal input results in relatively low Ras output in an analog manner.

(B) Inset: once a certain threshold in the analog receptor activation is surpassed, the output is characterized by digital Ras signals. Digital signals originate in the positive feedback loop that involves the allosteric pocket of SOS, initially primed by RasGTP coming from RasGRP, subsequently from both RasGRP and SOS.

(C) Previously stimulated cells maintain a limited period of increased sensitivity to activate Ras. The short-term hysteresis is caused by the low levels of RasGTP that remain but are potent

in engaging the allosteric feedback loop. Inset: short-term hysteresis provides a level of “signaling memory” in that a mild second signal can evoke a strong digital response because SOS molecules remain primed. However, hysteresis is limited and is lost long-term. The mechanisms of biochemical recruitment/retention of Grb2/SOS or RasGRP during hysteresis are unknown.

**Table 1**

Parameters used for the equations. Rates are calculated from the catalytic rates and/or the dissociation constants ( $K_D$ ) reported in the literature. For additional information see supplement, section I.

$k_1$	$k_{-1}$	$k_2$	$k_{-2}$	$k_3^{cat}$	$K_{3m}$	$k_4^{cat}$	$K_{4m}$	$k_5^{cat}$	$K_{5m}$
$1.8 \times 10^{-4} (\mu\text{m})^2 (\text{mols})^{-1} \text{s}^{-1}$ Sonderman et al. Cell (2004)	$3.0 \text{ s}^{-1}$ Sonderman et al. Cell (2004)	$1.7 \times 10^{-4} (\mu\text{m})^3 (\text{mols})^{-1} \text{s}^{-1}$ Sonderman et al. Cell (2004)	$0.4 \text{ s}^{-1}$ Sonderman et al. Cell (2004)	$0.038 \text{ s}^{-1}$ Freedman et al. PNAS (2006)	$1.64 \times 10^3 (\text{mols})/(\mu\text{m})^3$ Sonderman et al. Cell (2004) Freedman et al. PNAS (2006)	$0.003 \text{ s}^{-1}$ Boykevich et al. Curr. Biol. (2006)	$9.12 \times 10^2 (\text{mols})/(\mu\text{m})^3$ Sonderman et al. Cell (2004) Boykevich et al. Curr. Biol. (2006)	$0.1 \text{ s}^{-1}$ Gideon et al. Mol. Cell. Biol. (1992) Trahey et al. Science (1987)	$1.07 \times 10^2 (\text{mols})/(\mu\text{m})^3$ Gideon et al. Mol. Cell. Biol. (1992) Trahey et al. Science (1987)